

# The effect of powder forming method on the pull-out flaw populations observed on polished surfaces of alumina ceramics

Orhan Dengiz<sup>a</sup>, Tiandan Chen<sup>b</sup>, Ian Nettleship<sup>b,\*</sup>, Alice E. Smith<sup>a</sup>

<sup>a</sup> Department of Industrial and Systems Engineering, Auburn University, Auburn, AL 36849, United States

<sup>b</sup> Department of Materials Science and Engineering, University of Pittsburgh, Pittsburgh, PA, United States

Received 19 January 2006; received in revised form 31 March 2006; accepted 17 April 2006

## Abstract

Quantitative image analysis was used to study the effect of the powder forming method on the population of pull-out flaws for polished surfaces of dense alumina ceramics. By comparing the area fractions, the size distributions and the extreme values of the pull-out areas it was concluded that slip casting with dispersed slips resulted in significantly fewer and smaller pull-outs compared to slip casting with flocculated slips or powder pressing. The implications of these observations for the effect of the powder forming method on the strength of alumina ceramics are discussed. © 2006 Elsevier B.V. All rights reserved.

*Keywords:* Ceramic; Pull-out; Flaw population; Extreme value

## 1. Introduction

The effects of processing conditions on the properties of ceramics have been the subject of considerable study. Reports of the effect of processing and structure on the mechanical strength of ceramics extends back beyond early studies of the effect of grain size [1,2]. Implicit in this association is a correlation between the average grain size and the largest flaw size in the material, since the latter is assumed to ultimately result in failure. This approach was followed by studies that considered the more obvious relationships between the fracture strength and surface condition achieved through grinding the tensile surface of test specimens. The expected effect of grinding on fracture strength was observed, thereby confirming that the surface flaws were the common sources of failure [3]. More recent studies have looked at the effect of grinding on fracture strength, and linked the fracture strength to residual stress induced by machining [4] and the type of machining method used [5]. Correlations have also been made between the powder processing method used to form the ceramic and its fracture strength and Weibull modulus. This is easy to understand for pressing of granulated powders where the survival of a few granules can create large defects in the material [6]. However, correlations have also been discov-

ered between strength and different processing methods, based on observations of a population of intrinsic “volume defects” [7]. Although this population has not been directly quantified, the use of gel-casting to reduce the frequency of the volume defects caused a pronounced increase in strength from the range 450–600 MPa to values higher than 800 MPa [7].

Although correlations between the processing method and the fracture strength have proven instructive, a more direct comparison between the processing method and the flaw population is lacking. Many studies have examined the fracture origins after the strength tests to observe the nature of the flaw that was responsible for failure [8]. There have also been qualitative ranking of processing defects in terms of their propensity to reduce the fracture strength of ceramics [9]. Unfortunately, these approaches do not provide quantitative statistical information on which firm correlations can be based. This study was designed to develop a direct and quantitative ranking of the effect of the powder forming method on the pull-out flaw population on polished surfaces of alumina ceramics that were sintered for 5 and 10 h at 1350 °C. The surfaces were given the same grinding and polishing treatment so that differences in the pull-out population could be attributed to the powder forming technique. The analysis of the results relies on the assumption that the polished surfaces are representative sections and therefore comprises a random sampling of representative volumes. Under these conditions, the flaw populations are directly comparable. The sections were polished to avoid effects related to residual stresses induced by grinding

\* Corresponding author. Tel.: +1 412 624 9720; fax: +1 412 624 8069.  
E-mail address: nettles@pitt.edu (I. Nettleship).

under high loads. These residual stresses have been shown to control the fracture strength of ceramics [4]. The methods used in this study required images of the surfaces that could be automatically thresholded to capture the microstructural features. This would be difficult to apply to ground surfaces due to the topological contrast.

## 2. Experimental procedures

Cast samples were prepared using slips in both the dispersed condition and the flocculated condition. The dispersed slip was prepared by adding 1.7 ml of an ammonium polyacrylate dispersant (Darvan C, R.T. Vanderbilt Co., Norwalk, CT) to deionized water. Then, 50 g of alumina powder (Alcoa A-16SG, Pittsburgh, PA) was added to give a solid loading of 20 vol.%, before the slip was ball milled for 24 h without media and cast into a plaster mold. The flocculated sample was prepared by adjusting the pH of deionized water to pH 9 with ammonium hydroxide and then adding 50 g of the same alumina powder to give 20 vol.% solids followed by stirring for a few hours prior to casting into a plaster mold. The casts made with the two different slip dispersions will be referred to as the “dispersed” and the “flocculated” samples to simplify the discussion. Both samples were allowed to dry in room air for approximately 7 days. It was difficult to measure the green density of the samples due to their irregular shape, however, a previous study which used the same processing methods gave a green density of 62% for the dispersed material and a green density of 55% for the flocculated material [10]. The samples were then sintered at 1350 °C for 0.1 h using a heating rate of 5 °C/min and a cooling rate of 10 °C/min. Samples weighing a few grams were machined from the center of the casts. Archimedes density measurements, in which the samples were evacuated before immersion in water, showed that the density of samples cut from the same cast did not vary by more than 2%. Finally, the samples were sintered at 1350 °C to give total isothermal sintering times of 5 or 10 h using a heating rate of 5 °C/min and a cooling rate of 10 °C/min.

Samples of the same alumina powder were also uniaxially pressed in a 12.5 mm diameter die, without granulation, using a pressing pressure of 54 MPa. They were then sintered at 1350 °C for 5 and 10 h using a heating rate of 5 °C/min and a cooling rate of 10 °C/min. The green density of the pressed samples was 57%.

All the samples' sections were prepared and imaged under the same conditions. First, the sintered samples were sectioned and vacuum mounted in a low viscosity resin. Care was taken to make sure the all the sample sections received the same preparation conditions. They were flattened with a 30  $\mu\text{m}$  diamond impregnated wheel for 5 min followed by pre-polishing with 15  $\mu\text{m}$  diamond on a napless nylon cloth for 15 h and then polishing with 6  $\mu\text{m}$  for 3–4 h followed by 1  $\mu\text{m}$  diamond for 1–2 h, both using napless nylon cloths. Each sample section was then observed at  $\times 100$  magnification using bright field optical microscopy under identical illumination conditions. Either 19 or 20 images were taken at random locations on the sections. The approximate location of each field of view was recorded using the stage scale. This was done to check that the images

did not overlap and to make sure there were no trends in the spatial distribution of the features in the sections. The images were then processed by two methods that used Scion Image software (<http://www.scioncorp.com>). The first was a manual method that involved thresholding the pull-out flaws, which were dark relative to the surrounding ceramic. Each pull-out on the processed image was directly compared with the same pull-out on the original image to make sure it was faithfully represented. The resulting processed images were manually corrected by eliminating stray pixels and correcting any misrepresentation of any of the pull-outs. Fig. 1(a) shows an original image that can be compared with the manually processed image in Fig. 1(b). This processing procedure requires some operator interpretation so an automated algorithm [11] was developed for “adaptive thresholding” of the images. This method involved taking several images from the entire set taken in the study and manually recovering the pull-out features, while recording the density slice parameter values. Background equalization of the images was not done prior to the application of the adaptive thresholding procedure. Regression analysis was then used to develop an estimation function for the best density slicing parameters. The input variables were the average, standard deviation, minimum and maximum of the gray levels and the output variables were the density slice limits. The final image processing step involved a size filter which removed all the features less than 6 pixel, thereby eliminating stray pixels which appeared after manual thresholding due to local illumination conditions. Each pixel was 1.1  $\mu\text{m}^2$  and the largest pores in the distribution associated with sintering were 1  $\mu\text{m}^2$  so the filter was also large enough to eliminate any of pores associated with sintering and restrict the analysis to pull-out damage. The results of this automated method are shown in Fig. 1(c). Comparison of Fig. 1(b) and (c) shows some differences. For the larger pull-outs, the difference between the manual method and the automatic method were mostly caused by contrast difference within individual pull-outs due to their irregular shape. Lowering the gray scale of the threshold might improve the situation for some pores but not for others. Additionally, a lowering of the threshold gray scale will also result in the detection of “false flaws” caused by local illumination conditions. To avoid these issues and eliminate operator sensitivity, the automatic method was set to capture the darkest contrast. This is not thought to bias the statistical comparison since the flaws are considered to be roughly equiaxed and randomly oriented in the surface. The automatic method developed here also had the advantage that it was much less time consuming than the manual method.

### 2.1. Statistical analysis

Once the images had been processed, they were analyzed by focusing on three different statistical measurements. An assumption common to all of these measurements, as well as to all other quantitative image analysis studies, is that the polished section is a random section through a representative volume that does not contain any systematic gradients in the microstructure. As mentioned earlier, the approximate position of each pull-out feature on the surface was recorded and there appeared to be no evidence of systematic variation in the spatial distribution in any of the

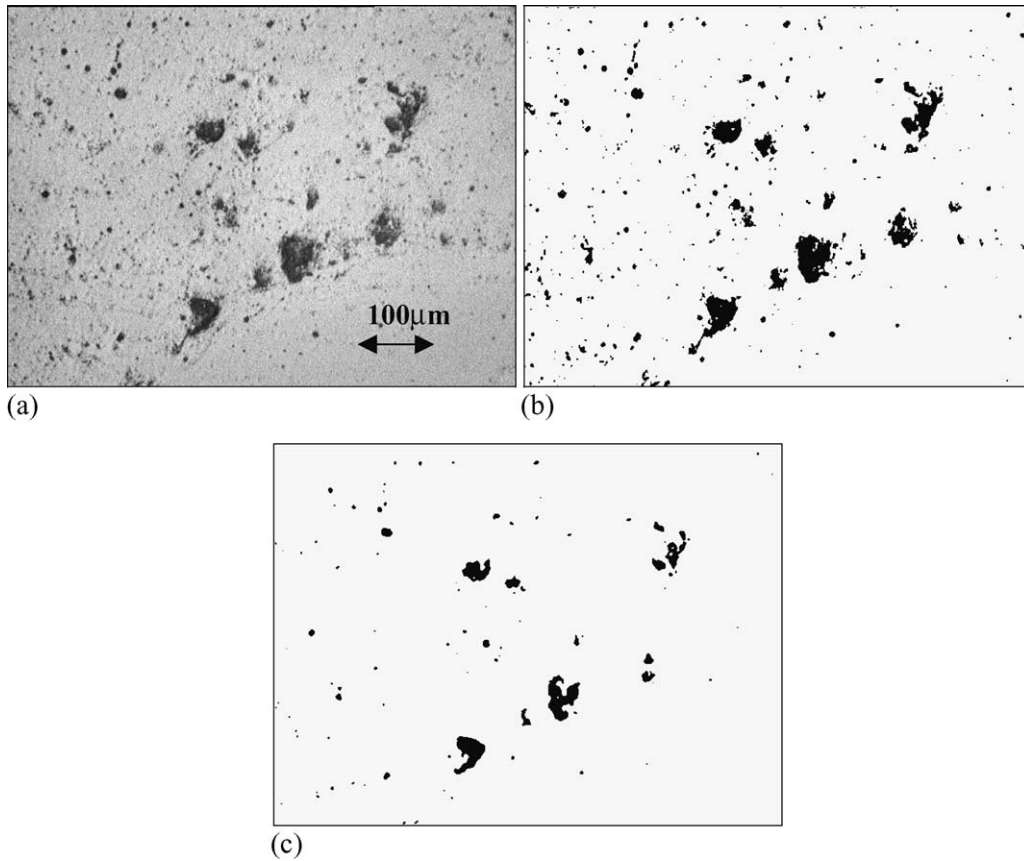


Fig. 1. (a) an example of an optical micrograph showing pull-out flaws; (b) shows the manually cleaned and thresholded image; and (c) the results of the automated image processing method used in this study.

samples. The first measurement undertaken was the area fraction of the pull-outs, with the 95% confidence interval being calculated based on the variation between the images. The second was the number frequency distribution in areas of the pull-outs. No attempt was made to unfold the pull-out size distribution into three dimensions for the purposes of this comparison. Finally, extreme value analysis was used to estimate the largest pull-out on the sections since these pull-outs might be expected to be those that control the fracture strength of the material. Extreme value analysis has been applied to a wide range of problems in which rare events of large or small magnitude occur at very low frequencies and result in a limited number of observations. The Generalized Pareto Distribution (GPD) is a flexible and widely applied limit distribution whose cumulative distribution function is given in Eq. (2). The spectrum of applications includes modeling high risks in financial markets [12] earthquake magnitudes [13] heavy winds [14,15,16] floods [12] particle size distributions [17] and maximum inclusion size in clean steel [18–21]. The Pareto law with a shape parameter  $\gamma$ , scale parameter  $s$ , and a location parameter  $\nu$  can be stated as:

$$1 - F_x(x) = \Pr\{X > x\} = \left(\frac{x - \nu}{s}\right)^{-1/\gamma}, \quad \gamma > 0, x \geq \nu \quad (1)$$

where  $X$  is the random variable,  $F_x(x)$  the cumulative probability function of  $X$ , i.e.  $F_x(x) = \Pr\{X < x\}$ . Pickands shows that the conditional cumulative distribution function,  $F_u(y)$ , of values of  $X$  over a large threshold  $u$ ,  $Y = X - u$ , is well approximated by the GPD for a large class of underlying distribution functions [22]. Dargahi-Noubary recommends GPD for use as the distribution of the excess of observed values over a certain threshold, as the threshold increases toward the right hand tail [14]. Also, Gilli and Kellezi provide detailed information on the GPD [12] from which Eqs. (2) and (3) can be derived.

$$F_u(y) \sim G_{\xi, \sigma}(y), \quad u \rightarrow \infty$$

$$P(Y \leq y | Y > 0) = G_{\xi, \sigma}(y) = \begin{cases} 1 - \left(1 + \frac{\xi}{\sigma} y\right)^{-1/\xi} & \text{if } \xi \neq 0 \\ 1 - e^{-y/\sigma} & \text{if } \xi = 0 \end{cases} \quad (2)$$

for  $0 \leq y \leq (x_{\max} - u)$ , is the Generalized Pareto Distribution. Where  $Y$  is the excess amount of  $X$  over the threshold  $u$ , and  $G_{\xi, \sigma}(y)$  the probability that the excess amount  $Y$  is less than or equal to  $y$  given that  $Y$  is greater than zero, and  $x_{\max}$  the maximum observed value of  $X$ .  $\xi$  is the shape parameter and  $\sigma$  the scale parameter. Since  $Y = X - u$ ,  $x$  can be defined as  $u + y$ , hence  $F(x)$  is the probability that the random variable  $X$  is less than or equal

to  $x$  given that it is larger than the threshold  $u$  as:

$$P(X < x | X > u) = F(x) = G_{\xi, \sigma}(x - u) \\ = 1 - \left(1 + \xi \frac{(x - u)}{\sigma}\right)^{-1/\xi} \quad (3)$$

The cases where  $\xi > 0$ ,  $\xi = 0$ , and  $\xi < 0$  correspond to Fréchet, Gumbel and reverse Weibull domains of attraction, respectively [13,15,16]. If there is theoretical or scientific evidence that there is a certain upper bound for  $x$ , then  $\xi < 0$  is used, else  $\xi > 0$  is used. Eqs. (2) and (3) are the conditional cumulative distribution of excess  $Y = X - u$  given  $Y > 0$  or  $X$  given  $X > u$ , respectively, for a sufficiently large threshold  $u$ .

### 3. Results and discussion

#### 3.1. The effect of sintering time and forming method on the area fraction of pull-out flaws

The solid volume fractions ( $V_s$ ) of the sintered samples are given in Table 1, along with the area fractions (AF) of the pull-outs on the polished surfaces. As expected, the flocculated samples, which had the lowest green density, had the lowest sintered solid volume fraction: 0.87 after 5 h and 0.9 after 10 h. The pressed and the dispersed samples both had solid volume fractions in the range of 0.94–0.96 after 5 and 10 h. Consideration of the area fraction showed that the pull-outs occupied less than 1% of the analyzed area in all samples. However, the area fractions of the pull-outs in the dispersed samples were close to an order of magnitude less than the area fraction of pull-outs in the flocculated and the pressed samples. For the dispersed samples, the increase in the area fraction of the pull-outs with increasing sintering time is not significant according to the confidence intervals. In contrast, the pressed samples showed a significant increase in the area fraction of pull-outs from 0.002 to 0.008 when the sintering time was increased. Finally, the area fraction of pull-outs did not change for the flocculated sample, the values for both sintering times being 0.005. The range of the confidence intervals did not allow clear ranking of the flocculated and the pressed condition. However, the area fraction results do suggest that there is less pull-out in the dispersed samples. This might be associated with the fact that slip casting with dispersed slips not only results in better particle packing and higher green density,

but also results in fewer large packing defects that cause local differential sintering and result in pull-outs on machining of the sintered ceramic. While the area fraction of pull-outs might correlate with strength and reliability of ceramics, one would expect that there would be a more direct link with the size distribution of pull-outs. Therefore, the characteristics of the size distribution must be considered.

#### 3.2. The effect of processing condition on pull-out flaw size distribution

Fig. 2 shows the cumulative number frequency distribution of the areas of the pull-outs for sintering times of 5 and 10 h. Note the data was collected as discrete cumulative histograms but they are shown in the figures as continuous best-fit curves through the data points. The low magnification optical microscopy ensured that the distribution contained large features that are thought to be associated with pull-out damage on machining. The areas of the pull-outs were much larger than the areas of the pores that developed during sintering. The distribution in pore areas associated with sintering of similarly processed materials commonly extended from 0.01 to  $1 \mu\text{m}^2$  with a mean value of approximately  $0.1 \mu\text{m}^2$  [23]. It is possible that some of the largest pores that survive sintering could contribute to the smallest size intervals in the distribution of pull-outs measured in this study. As mentioned in the procedures section, the 6 pixel filter removed these pores and restricted the analysis to the pull-out populations.

The comparison of the area distributions in Fig. 2(a) shows that the dispersed sample had smaller pull-outs after 5 h of sintering, with areas extending from 6 to  $62 \mu\text{m}^2$  approximately. For the pressed and the flocculated materials, the size distribution extended up to approximately 623 and  $1108 \mu\text{m}^2$ , respectively. Clearly, the forming method significantly affects the size distribution of the pull-outs. It is interesting to note that a ranking of the processing methods by the mean of the pull-out area from largest to smallest would result in the same ranking of the processing methods based on green density when ranked from lowest to highest. It is therefore possible to speculate that the packing of the powder particles not only controls the green density but also affects the formation of defects that result in pull-outs on machining, grinding and polishing of the surfaces. When the sintering time was increased to 10 h, Fig. 2(b) shows little effect on the distribution of the areas of the pull-outs for both the

Table 1

The effect of forming method and sintering time on the solid volume fraction ( $V_s$ ) of the sample and the area fraction (AF) of pull-outs on polished surfaces

	Method					
	Pressed		Flocculated		Dispersed	
	5.0	10.0	5.0	10.0	5.0	10.0
Duration (h)						
Sample size	19	20	20	20	20	20
$V_s$	0.94	0.95	0.87	0.90	0.94	0.96
AF lower CL <sup>a</sup>	0.001358	0.005039	0.003542	0.003982	0.000051	0.000090
AF average	0.002180	0.008129	0.005264	0.005130	0.000142	0.000323
AF upper CL <sup>a</sup>	0.003002	0.011218	0.006986	0.006278	0.000232	0.000557

<sup>a</sup> 95% confidence intervals.

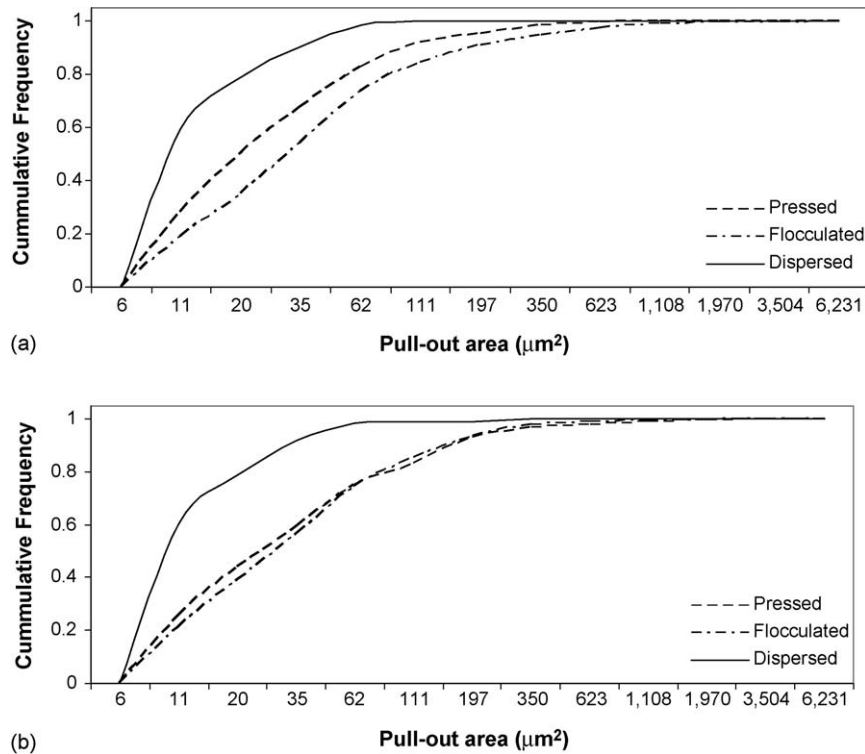


Fig. 2. (a) The number frequency distributions of the pull-out areas after sintering for 5 h. (b) The number frequency size distributions of the pull-out areas after sintering for 10 h.

dispersed and the flocculated samples. In fact, the distributions for the 5 and 10 h sintering times are almost identical. It can therefore be concluded that the increase in sintering time had no significant effect on either the area fraction or the size distributions of the pull-outs for the dispersed or the flocculated material. After sintering the pressed material for 10 h, the size distribution of the pull-outs moved to larger sizes and was much closer to the pull-out distribution of the flocculated sample sintered for the same time. This accompanies the increase in area fraction previously described for this material. The results suggest that the defects that result in pull-outs in the pressed material have grown with sintering time. Alternatively, the increase in the size of the defects could be affected by the growth of a microstructural feature, such as grain size, that is instrumental in the mechanism of pull-out formation. Indeed, this would be consistent with the effect of sintering time on grain size and past reports that have linked the thermal expansion anisotropy and the grain size of alumina to the level of residual stresses and microcracking in the microstructure [24]. Locally, high levels of residual stress in the microstructure could create the conditions for pull-out on machining. It is difficult to speculate further on this possibility without more systematic study of the effect of sintering time on the pull-out populations and the extent to which they correlate with microstructural populations. In particular, the reasons why this behavior was not observed for the dispersed or the flocculated materials need to be further investigated. More study will also be required concerning the mechanism by which the pull-outs are generated.

### 3.3. The effect of forming method on the extreme value of the pull-out flaws

For the purpose of the extreme value analysis, the data sets for the 5 and 10 h sintering times were combined in order to arrive at a ranking of the pressed, flocculated and dispersed processing conditions in terms of the areas of the largest pull-outs in the distributions.

Fig. 3 shows a comparison of the percentile plots for the GPD predictions. Each figure shows a direct comparison of the prediction for one forming method with the prediction for another forming method, as well as a lower and an upper estimate based on the 90% confidence interval. For the purposes of this study, the differences between the samples were considered significant if the upper estimate of one sample was below the lower estimate of the other. Fig. 3(c) shows that the prediction for the pressed samples is slightly smaller than the prediction for the flocculated samples at any given percentile in the upper 1% of pull-out areas. For example, the predicted area of the pull-outs at the 99.9 percentile is  $2523 \mu\text{m}^2$  for the pressed samples and  $2938 \mu\text{m}^2$  for the flocculated samples. However, the confidence intervals overlap so the differences in the predicted extreme value between the flocculated and the pressed samples are not considered significant. In contrast, Fig. 3(a) and (b) shows that the predicted extreme values for the largest 1% of the pull-outs in the dispersed samples are much smaller ( $134 \mu\text{m}^2$  at the 99.9 percentile) than for the flocculated or the pressed samples. In the case of Fig. 3(a) and (b), the confidence intervals in the comparisons do not over-

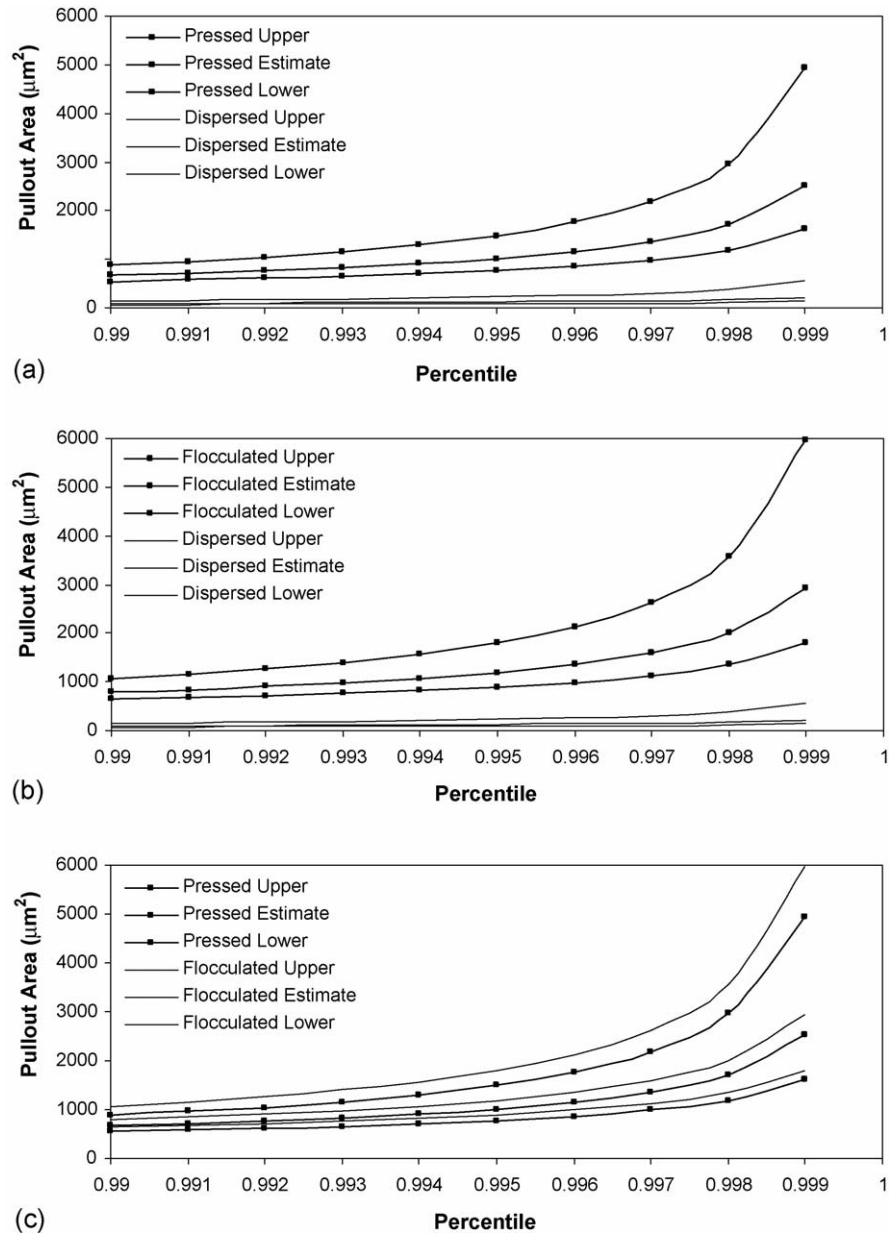


Fig. 3. (a) A comparison of the extreme value prediction for the pull-outs in the pressed and the dispersed samples. The upper and lower bounds of each estimate are based on the 90% confidence interval. (b) A comparison of the extreme value prediction for the pull-outs in the flocculated and the dispersed samples. The upper and lower bounds of each estimate are based on the 90% confidence interval. (c) A comparison of the extreme value prediction for the pull-outs in the flocculated and the pressed samples. The upper and lower bounds are based on the 90% confidence interval.

lap and it can be concluded that the dispersed condition resulted in smaller pull-outs. It is interesting to consider that the effect of the processing methods on the extreme value of the pull-out areas correlate with their effect on the area fractions and the size distributions of the pull-outs. All three measurements show that casting with a dispersed slip resulted in a significantly lower amounts of pull-out, and smaller pull-out flaws when compared with powder pressing and casting with flocculated slips.

While a comparison of mechanical properties was beyond the scope of this study, it is possible to estimate the effect of the extreme values of the pull-out areas on strength. First, it must be assumed that the largest pull-outs, the 99.9 percentile in this case, would be the strength controlling defects. The prediction

would assume that the pull-outs are strength controlling and the flaw size,  $c$ , can be approximated by the equivalent diameter. An estimate of the strength can then be made using the fracture toughness  $K_{IC}$ , for alumina. This has been shown to vary with grain size between 2 and 6 MPam<sup>0.5</sup>, and cannot strictly be considered to be a material constant [25]. However, for the purposes of this estimate, which simply ranks the processing methods by predicted strength, a value of 4 MPam<sup>0.5</sup> was assumed. The fracture strength  $\sigma_f$  is then given by Eq. (5):

$$\sigma_f = K_{IC} / \psi(\pi c)^{0.5} \tag{5}$$

where  $\psi$  is a constant equal to 1.12.

Table 2

The estimated equivalent diameter of the flaw sizes based on the estimated pull-out areas at the 99.9 percentile and the predicted strength of the ceramic

Method	Pressed	Flocculated	Dispersed
Estimated flaw size ( $\mu\text{m}$ )	57	61	13
Predicted strength (MPa)	267	258	559

Table 2 gives the values of the flaw size calculated from the extreme value analysis and the predicted strength. It is clear that the flaw sizes calculated from the extreme value analysis are large enough to affect the strength of fine grained aluminas. However, the extent to which they do so will depend on the volume of material under load in the test [26]. It is not surprising that the smaller pull-outs in the dispersed samples should result in a significantly higher predicted strength. Indeed, it is pertinent to point out that a similar strength increment, although not involving the same strength values, has been observed for gel-cast alumina compared to conventionally processed alumina [7]. This was attributed to the removal of large “volume flaws” by the superior particle packing achieved in the gel-cast samples. The findings of this study would support this explanation if the volume flaws resulted in pull-outs on the machined surfaces. Further investigations are required to improve our understanding of the nature of volume flaws and pull-outs and the mechanisms by which they are formed. This study also suggests that investigation of the populations of pull-out defects on machined surfaces could be used to quantitatively link the effect of ceramics processing to strength and reliability.

#### 4. Conclusion

The results of this study show that the population of pull-outs on machined and polished surfaces was influenced by the forming method used to process alumina ceramics. The samples made by casting with dispersed slips had a lower area fraction of pull-outs than samples made by powder pressing or casting with flocculated slips. The dispersed samples also exhibited smaller size distributions and a smaller extreme value of the pull-out areas.

#### Acknowledgements

The authors would like to thank the National Science Foundation for funding this project under award DMI 0301273. The

use of the facilities in the Materials Microcharacterization Laboratory at the University of Pittsburgh is also gratefully acknowledged.

#### References

- [1] W.D. Crandall, D.H. Chung, T.J. Gray, in: W.W. Kriegel, H. Palmour III (Eds.), *Mechanical Properties of Engineering Ceramics* Interscience, New York, 1961, pp. 349–379.
- [2] R.W. Davidge, G. Tappin, *J. Mater. Sci.* 3 (1968) 297–301.
- [3] R.C. Bradt, J.L. Dulberg, R.E. Tressler, *Acta Metall.* 24 (1976) 529–534.
- [4] W. Pfeiffer, T. Hollstein, *J. Euro. Ceram. Soc.* 23 (2003) 469–478.
- [5] L. Esposito, A. Tucci, G. Andalo, *J. Euro. Ceram. Soc.* 23 (2003) 479–486.
- [6] W.J. Walker, J.S. Reed, S.K. Verma, *J. Am. Ceram. Soc.* 82 (1999) 50–56.
- [7] A. Kreil, *J. Am. Ceram. Soc.* 81 (1998) 1900–1906.
- [8] G.D. Quinn, *Advances in ceramics*, in: J. Varner, V.D. Frechette (Eds.), *Fractography of Glasses and Ceramics*, vol. 22, American Ceramics Society, Westerville, OH, 1988, pp. 319–333.
- [9] F.F. Lange, *J. Am. Ceram. Soc.* 72 (1989) 3–15.
- [10] S.A. Schmidt, M.S. thesis, University of Pittsburgh, 1998.
- [11] O. Dengiz, A.E. Smith, I. Nettleship, *Int. J. Prod. Res.*, in press.
- [12] M. Gilli, E. Kellezi, An application of extreme value theory for measuring financial risk, Research paper, Preprint submitted to Elsevier Science, available online at: <http://www.unige.ch/ses/metri/gilli/evtrm/GilliKelleziEVT.pdf> (accessed 14 July 2005).
- [13] J. Caers, J. Beirlant, M.A. Maes, *Math. Geology* 31 (1999) 391–410.
- [14] G.R. Dargahi-Noubary, *Math. Geology* 21 (1989) 829–842.
- [15] E. Simui, N.A. Heckert, National Institute of Standards and Technology Building Science Series 174, NBSSES, Coden, 1995.
- [16] N.A. Heckert, E. Simui, T. Whalen, *J. Struct. Eng.* 124 (1998) 445–449.
- [17] D. Dierickx, B. Basu, J. Vleugels, O. Van der Biest, *Mater. Characterization* 45 (2000) 61–70.
- [18] G. Shi, H.V. Atkinson, C.M. Sellars, C.W. Anderson, *Acta Mater.* 47 (1999) 1455–1468.
- [19] C.W. Anderson, G. Shi, H.V. Atkinson, C.M. Sellars, *Acta Mater.* 48 (2000) 4235–4246.
- [20] G. Shi, H.V. Atkinson, C.M. Sellars, C.W. Anderson, J.R. Yates, *Acta Mater.* 49 (2001) 1813–1820.
- [21] C.W. Anderson, G. Shi, H.V. Atkinson, C.M. Sellars, J.R. Yates, *Acta Mater.* 51 (2003) 2331–2343.
- [22] J. Pickands III, *Ann. Stat.* 3 (1975) 119–131.
- [23] R.J. McAfee, I. Nettleship, *Acta Mater.* 53 (2005) 4305–4311.
- [24] S.J. Bennison, B.R. Lawn, *Acta Metall.* 37 (1989) 2659–2671.
- [25] P. Chantikul, S.J. Bennison, B.R. Lawn, *J. Am. Ceram. Soc.* 73 (1990) 2419–2427.
- [26] G.D. Quinn, R. Morrell, *J. Am. Ceram. Soc.* 74 (1991) 2037–2066.